Supporting Information

Zandany *et al.* 10.1073/pnas.0804104105

SI Text

Molecular Biology. We thank Fred Sigworth (Yale University, New Haven, CT) for kindly donating cDNA encoding the tandem *Shaker* Kv channel tetramer inserted into the pGEM vector (an 11-kb vector encoding for four channel subunits (≈2 kb each) along with their unique linkers) and for the four KS pBluscript plasmids (pBS), each encoding a Kv channel subunit [lacking the inactivation ball and chain domains (i.e., residues 4–29 deleted)], flanked by unique restriction sites. Principally, different combinations of mutated subunits were generated using a molecular LEGOing "cut-and-paste" technique, as described (1). Briefly, subunit mutations in *Shaker* channel cDNAs were introduced in the appropriate pBS plasmids by the QuikChange method (Stratagene) and confirmed by sequencing the entire cDNA. DNA encoding the mutated subunit was then cut by using the appropriate restriction enzymes and ligated into the vector encoding the tandem tetrameric channel, precut with the same restriction enzymes to remove the wild-type subunit of choice. PCR amplification using appropriate (linkers-flanking) primers was performed to select for colonies harboring DNA encoding the tandem tetrameric channel. After selection of a positive colony, verification of the insertion of the mutated subunit-encoding gene, especially in two-way ligations involving 2- and 9-kb DNA fragments, was achieved when the putative mutated subunit of the tandem channel tetramer cDNA was amplified by using standard PCR after isolation of the DNA fragment containing the mutation site, by using the appropriate restriction enzymes. The amplified DNA fragment was then cloned into a T vector, and the insertion of the mutation was reverified by direct sequencing. Different combinations of mutated subunits of the tandem tetrameric channel were achieved by either two- or three-way ligations of cDNAs encoding for one or two wild-type or mutant subunits (2 + 2 + 7 or 2 + 4 + 5 kb fragments for the three-way ligation or 4 + 7-kb fragments for the two-way ligation) precut with the appropriate restriction enzymes.

Data Analysis. Voltage-activation curves were generated by using measured tail currents and fitted by using the Origin program (version 5, Microcal Software) to a two-state Boltzmann equation: $I/I_{max} = (1 + e^{-ZF(V-V_{1/2})/RT})^{-1}$, where I/I_{max} is the normalized tail current amplitude for the *Shaker* channels, Z is the activation slope factor, $V_{1/2}$ the half activation voltage, and T, F, and R have their usual thermodynamic meanings. Free-energy differences between closed (C) and open (O) states of the wild type or mutant subunit channels were parameterized based on the gating shifts and slopes, according to $ZFV_{1/2}$ ($= -RT\ln[O]/[C]$). Standard errors in $ZFV_{1/2}$ and $\Delta(ZFV_{1/2})$ ($= F(Z_{wt}\,V_{1/2\,wt} - Z_m\,V_{1/2m})$) were calculated by standard linear error propagation.

High-Order Intersubunit Coupling Analysis. Higher-order thermodynamic coupling analysis was performed as described in detail (2, 3). Briefly, the second-order (pairwise) intersubunit coupling free energy between two channel subunits, i and j [$\Delta^2G_{(i,j)}$], was calculated by using a simple thermodynamic square comprising the wild-type protein, the two single-subunit mutants, and the corresponding double-subunit mutant (Fig. 1*B*) (4). In such a cycle, the free energy changes upon mutation of subunit i in the presence (ΔG_1) or absence (ΔG_2) of a similar mutation in subunit j are compared. If the free-energy change of mutating subunit i is independent of the presence or absence of a similar mutation in subunit j, then the two subunits are not coupled ($\Delta G_1 = \Delta G_2$). Otherwise, they are coupled, and the free energy of intersubunit interaction, $\Delta^2G_{(i,j)}$, is expressed by $\Delta G_1 - \Delta G_2$. Third-order intersubunit coupling free energies [$\Delta^3G_{(i,j)k}$], reflecting the energetic effect of a third subunit, k, on the intersubunit coupling free energy between the (i,j) subunit pair, were calculated by using a three-dimensional cubic construct, as described in ref. 3 (see figure 2*B* therein). The front and back faces of such a cube are double-mutant cycles used to measure the coupling free energy between the i and j subunits in the absence and presence of a similar mutation in the third subunit (k), respectively. Subtracting the intersubunit coupling free energies calculated for each of these cycles gives a quantitative measure for the effect of a third subunit (k) on the interaction between two adjacent subunits (i,j) (2). Fourth-order intersubunit coupling free energies [$\Delta^4G_{(i,j)(k,l)}$], reflecting the energetic effect of the interaction between the (k,l) subunit pair on the intersubunit coupling free energy between the (i,j) subunit pair, were calculated by using a four-dimensional (4D) construct (double-mutant cycle of double-mutant cycles), as described in ref. 3 (see figure 3*A* therein). At the corners of such a construct are the double-mutant cycles used to measure the intersubunit interaction energies between the i and j subunits in the absence of any further subunit mutation (upper left corner of the 4D construct) or in the presence of a similar single-subunit mutation (upper right and lower left corners of the 4D construct) or double (lower right corner of the 4D construct) subunit mutations. Values and errors for the nth-order intersubunit coupling free energies were calculated essentially as described.

Intersubunit Coupling Dataset. Eleven different intersubunit double-mutant cycles were analyzed in the present study. Of the 11 pairs, 6 were between the different possible (pairwise) subunit combinations of a tetrameric protein, in the absence of any other mutation in adjacent subunits, 4 pairs were between subunit pairs in the presence of another adjacent subunit mutation, and a single pair was between subunits against the background of a double-subunit mutation. From these 11 cycles, six second-order intersubunit coupling terms [$\Delta^2G_{(i,j)}$], four third-order intersubunit coupling terms [$\Delta^3G_{(i,j)k}$], and one fourth-order coupling term [$\Delta^4G_{(i,j)(k,l)}$] were obtained.

1. Yang Y, Yan Y, Sigworth FJ (1997) How does the W434F mutation block current in *Shaker* potassium channels? *J Gen Physiol* 109:779–789.
2. Horovitz A, Fersht AR (1990) Strategy for analyzing the co-operativity of intramolecular interactions in peptides and proteins. *J Mol Biol* 214:613–617.
3. Sadovsky E, Yifrach O (2007) Principles underlying energetic coupling along an allosteric communication trajectory of a voltage-activated K^+ channel. *Proc Natl Acad Sci USA* 104:19813–19818.
4. Horovitz A (1996) Double-mutant cycles: A powerful tool for analyzing protein structure and function. *Fold Des* 1:R121–R126.

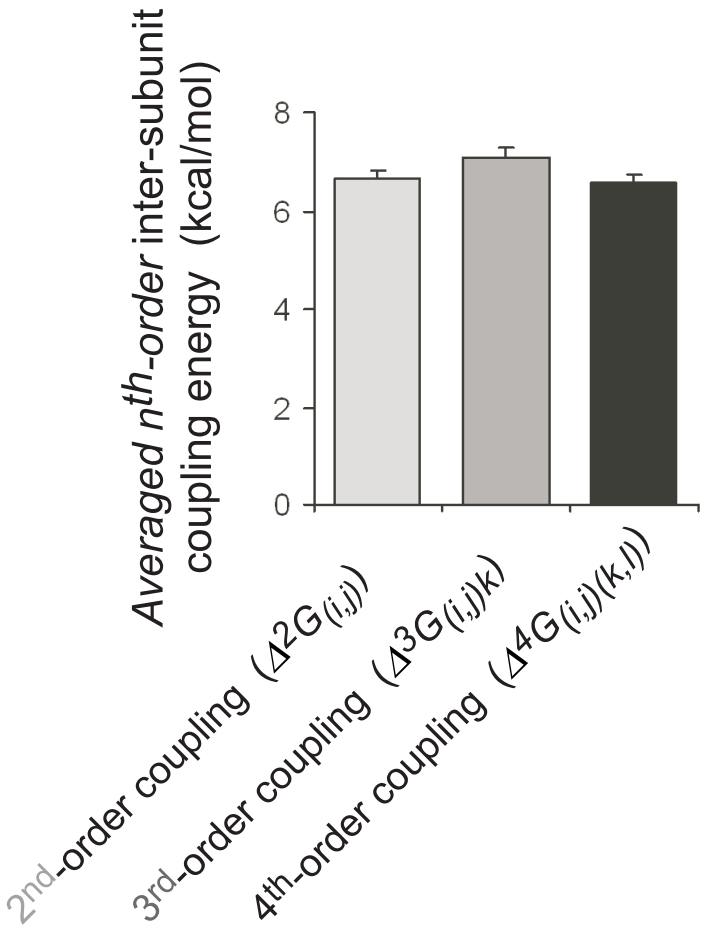

Fig. S1. Comparison of the average high-order intersubunit coupling free energies for the six subunit interactions indicated in Fig. 4*B*. All high-order intersubunit coupling values are listed in Tables S2–S4.

Table S1. The influence of different combinations of the G466P subunit mutation on voltage-dependent gating of the *Shaker* K^+ channel

Channel protein	$V_{1/2}$, mV	Z	ΔG_{open}, kcal/mol
w^4*	−26.5 ± 0.2	3.20 ± 0.08	−1.97 ± 0.01
wwww	−24.3 ± 0.1	3.07 ± 0.12	−1.73 ± 0.01
mwww (A)	−61.6 ± 0.2	5.70 ± 0.25	−8.15 ± 0.04
wmww (B)	−59.2 ± 0.1	5.85 ± 0.18	−8.03 ± 0.03
wwmw (C)	−57.0 ± 0.2	5.66 ± 0.27	−7.48 ± 0.04
wwwm (D)	−60.9 ± 0.2	5.60 ± 0.27	−7.91 ± 0.04
mmww (AB)	−60.0 ± 0.3	5.20 ± 0.14	−7.24 ± 0.04
mwmw (AC)	−65.1 ± 0.3	4.77 ± 0.21	−7.20 ± 0.04
mwwm (AD)	−63.9 ± 0.1	5.52 ± 0.23	−8.17 ± 0.04
wmmw (BC)	−65.6 ± 0.2	4.78 ± 0.20	−7.27 ± 0.04
wmwm (BD)	−59.7 ± 0.2	5.15 ± 0.14	−7.13 ± 0.02
wwmm (CD)	−62.1 ± 0.2	5.17 ± 0.20	−7.45 ± 0.03
mmmw (ABC)	−64.6 ± 0.2	5.44 ± 0.23	−8.14 ± 0.04
mmwm (ABD)	−68.9 ± 0.1	4.11 ± 0.08	−6.57 ± 0.02
mwmm (ACD)	−64.4 ± 0.2	4.86 ± 0.12	−7.26 ± 0.03
wmmm (BCD)	−63.0 ± 0.1	5.10 ± 0.07	−7.45 ± 0.01
mmmm (ABCD)	−63.6 ± 0.2	5.57 ± 0.11	−8.22 ± 0.02
m^4*	−67.2 ± 0.1	5.75 ± 0.12	−8.96 ± 0.02

Presented are gating parameters of all single-, double-, triple- and quadruple-mutant subunit combinations used to calculate the intersubunit coupling free energies presented in Fig. 4 and listed in Table S2.

*w^4 and m^4 denote the respective tetrameric wild-type and G466P mutant channel proteins assembled from four identical monomers.

Table S2. Second-order intersubunit coupling free energies of all pairwise subunit combinations of the tetrameric *Shaker* Kv channel

(*i*, *j*) Subunit pair*	$\Delta^2G_{(i,j)}$, kcal/mol
(A,B)	7.21 ± 0.06
(A,C)	6.69 ± 0.07
(A,D)	6.15 ± 0.08
(B,C)	6.51 ± 0.07
(B,D)	7.08 ± 0.05
(C,D)	6.21 ± 0.07

*The coupling free energy of the (*i,j*) subunit pair, as also indicated in Fig. 4*A*, was measured as described in SI *Text*.

Table S3. Third-order intersubunit coupling free energies for the tetrameric *Shaker* Kv channel

(*i, j*)*k* Subunit triad*	$\Delta^2G_{(i,j)}$, kcal/mol native *k*	$\Delta^2G_{(i,j)}$, kcal/mol mutated *k*	$\Delta\,^3G_{(i,j)k}$, kcal/mol†
(A,B) C‡	7.21 ± 0.06	−1.14 ± 0.08	8.35 ± 0.10
(A,B) D	7.21 ± 0.06	0.82 ± 0.06	6.39 ± 0.08
(A,C) D	6.69 ± 0.07	0.44 ± 0.07	6.25 ± 0.11
(B,C) D	6.51 ± 0.07	−0.78 ± 0.06	7.29 ± 0.09

*The coupling free energy of the (*i,j*) subunit pairs was measured in the presence or absence of the native or G466P-mutated third *k* subunit (see SI *Text*).
†The effect of subunit *k* on the (*i,j*) intersubunit interaction pair is calculated by subtracting the free energies of intersubunit coupling in the presence or absence (mutated) of the native third subunit (see refs. 1 and 2 below).
‡Considering the symmetry of the three-dimensional mutant construct (a thermodynamic cube), examining any of the three pairwise subunit combinations of a subunit triad in the presence and absence of the third native subunit yields a similar value for $\Delta\,^3G_{(i,j)k}$ (1, 2).

1. Horovitz A, Fersht AR (1990) Strategy for analyzing the co-operativity of intramolecular interactions in peptides and proteins. *J Mol Biol* 214:613–617.
2. Sadovsky E, Yifrach O (2007) Principles underlying energetic coupling along an allosteric communication trajectory of a voltage-activated K^+ channel. *Proc Natl Acad Sci USA* 104:19813–19818.

Table S4. Fourth-order intersubunit coupling free energy for the tetrameric *Shaker* Kv channel

(*i, j*) (*k, l*) Subunit quadruple*	$\Delta^2G_{(i,j)}$, kcal/mol native *k* and *l* 1	$\Delta^2G_{(i,j)}$, kcal/mol mutated *k*, native *l* 2	$\Delta^2G_{(i,j)}$, kcal/mol native *k*, mutated *l* 3	$\Delta^2G_{(i,j)}$ kcal/mol mutated *k* and *l* 4	$\Delta\,^4G_{(i,j)(k,l)}$, kcal/mol†
(A,B) (C,D)‡	7.21 ± 0.06	−1.14 ± 0.08	0.82 ± 0.06	−0.95 ± 0.05	6.58 ± 0.13

*The coupling free energy of the (*i,j*) subunit pair was measured in the absence of any other subunit mutation (native *k* and *l*) or in the presence of either the *k* or *l* G466P-mutated third subunit or on the background of the double mutant where both *k* and *l* subunits bear the G466P mutation (see *Materials and Methods*).

†The effect of the (*k,l*) intersubunit interaction on the (*i,j*) intersubunit interaction pair is calculated by subtracting the free energies of intersubunit coupling according to (1–2)–(3–4) as previously described (see refs. 1 and 2 below).

‡Considering the symmetry of the four-dimensional mutant construct (double-mutant cycles of double-mutant cycles), examining the context-dependence any of the six possible pairwise subunit combinations of a subunit quadruple yields a similar value for $\Delta\,^4G_{(i,j)(k,l)}$ (1, 2).

1 Horovitz A, Fersht AR (1990) Strategy for analyzing the co-operativity of intramolecular interactions in peptides and proteins. *J Mol Biol 214:613–617.*

2. Sadovsky E, Yifrach O (2007) Principles underlying energetic coupling along an allosteric communication trajectory of a voltage-activated K^+ channel. *Proc Natl Acad Sci USA* 104:19813–19818.